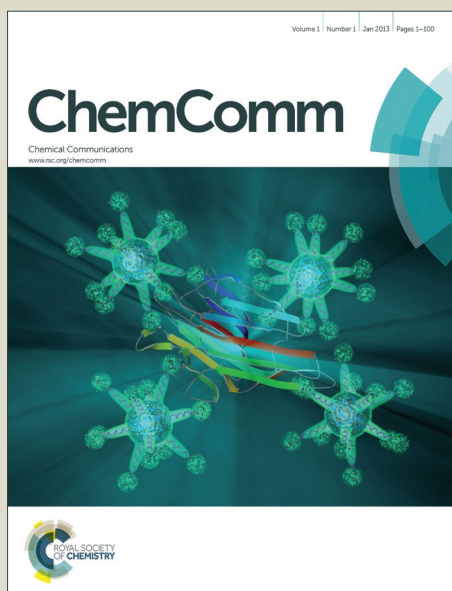


# ChemComm

Accepted Manuscript



This is an *Accepted Manuscript*, which has been through the Royal Society of Chemistry peer review process and has been accepted for publication.

*Accepted Manuscripts* are published online shortly after acceptance, before technical editing, formatting and proof reading. Using this free service, authors can make their results available to the community, in citable form, before we publish the edited article. We will replace this *Accepted Manuscript* with the edited and formatted *Advance Article* as soon as it is available.

You can find more information about *Accepted Manuscripts* in the [Information for Authors](#).

Please note that technical editing may introduce minor changes to the text and/or graphics, which may alter content. The journal's standard [Terms & Conditions](#) and the [Ethical guidelines](#) still apply. In no event shall the Royal Society of Chemistry be held responsible for any errors or omissions in this *Accepted Manuscript* or any consequences arising from the use of any information it contains.

Journal Name

COMMUNICATION

## Enantioselective Adsorption in Homochiral Metal-Organic Frameworks: The Pore Size Influence

 Received 00th January 20xx,  
 Accepted 00th January 20xx
Zhi-Gang Gu,<sup>a</sup> Sylvain Grosjean,<sup>b</sup> Stefan Bräse,<sup>c</sup> Christof Wöll,<sup>a</sup> Lars Heinke<sup>a,\*</sup>

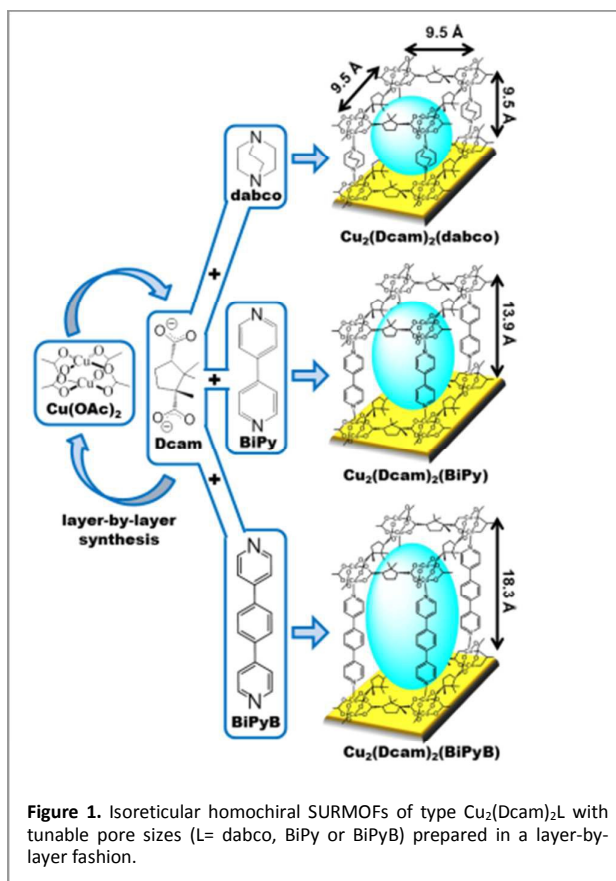
DOI: 10.1039/x0xx00000x

www.rsc.org/

**Abstract** Uptake experiments in thin films of isorecticular chiral MOFs of type  $\text{Cu}(\text{Dcam})(\text{L})$  with identical stereogenic centers but different pore dimensions show that the enantioselectivity is significantly influenced by the pore size. The highest selectivity was found for medium pore sizes, roughly corresponding the extension of the chiral guest molecule, limonene.

the adsorption capacity and also on the selectivity of achiral MOFs.<sup>20-22</sup> A few publications<sup>23-27</sup> investigate the enantioselectivity of different chiral MOFs with tunable structures, however, a systematic study of the impact of the pore size of the chiral MOFs on the enantioselectivity has not yet been carried out. Here, we investigate the influence of the pore size of isorecticular chiral MOFs (i.e. of MOFs with the same topology and identical stereogenic centers but with tunable pore sizes) on the enantioselectivity.

Enantiomer separation of chiral molecules is an important field of chemistry and has many important applications in pharmaceutical, agricultural and chemical engineering.<sup>1</sup> For instance, many pharmaceutical molecules are chiral and often only one enantiomer of the molecule has the desired effect, while the other enantiomer has negative side effects. An effective enantiomer separation is, therefore, necessary for virtually all applications of chiral molecules. Due to their large specific surface area and their regular, crystalline structure, homochiral metal-organic frameworks (MOFs) are very promising candidates for an efficient enantiomer separation.<sup>2-4</sup> MOFs are crystalline, nanoporous solids self-assembled from metal or metal-oxo clusters and organic ligands.<sup>5-7</sup> Since the first synthesis of homochiral MOFs in 1999,<sup>8</sup> the field has rapidly developed.<sup>2, 9-17</sup> Up to now, more than 30 different chiral MOFs have been used for investigating the enantioselective adsorption.<sup>4</sup> So far, the research was mainly of trial and error type. Guiding principles for understanding and optimizing the mechanism for enantiomer separation are virtually absent. It is obvious, and was shown in a number of papers<sup>2, 18, 19</sup> that the stereogenic center in the MOF structure has a significant impact on the enantiomeric excess. There are occasional reports that the pore size has a substantial impact on



<sup>a</sup> Dr. Z.G. Gu, Prof. Dr. C. Wöll, Dr. L. Heinke Institute of Functional Interfaces (IFG), Karlsruhe Institute of Technology (KIT), Hermann-von-Helmholtz-Platz 1, 76344 Eggenstein-Leopoldshafen, Germany  
 E-mail: Lars.Heinke@KIT.edu

<sup>b</sup> Dr. S. Grosjean, Institute of Biological Interfaces (IBG), Karlsruhe Institute of Technology (KIT), Hermann-von-Helmholtz-Platz 1, 76344 Eggenstein-Leopoldshafen, Germany

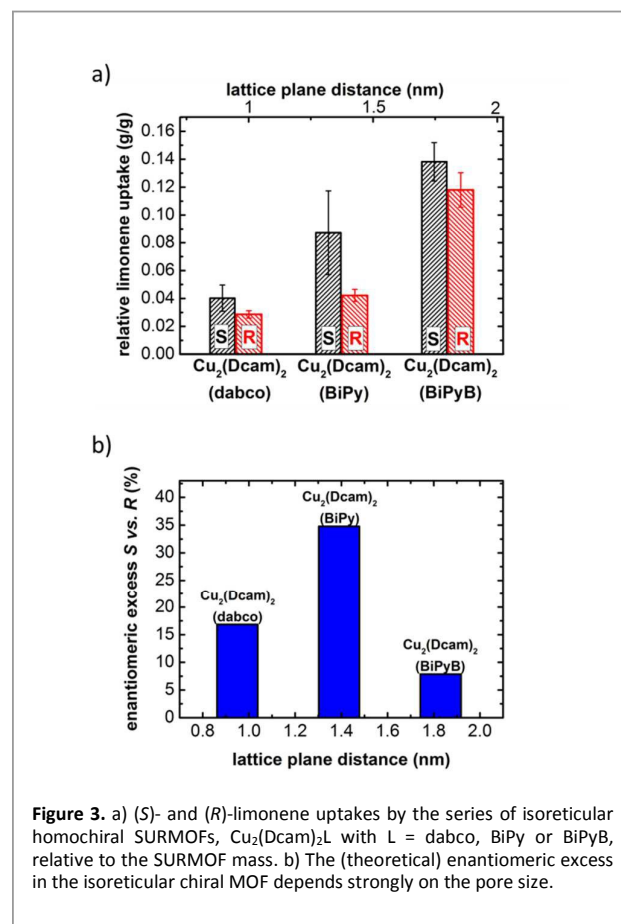
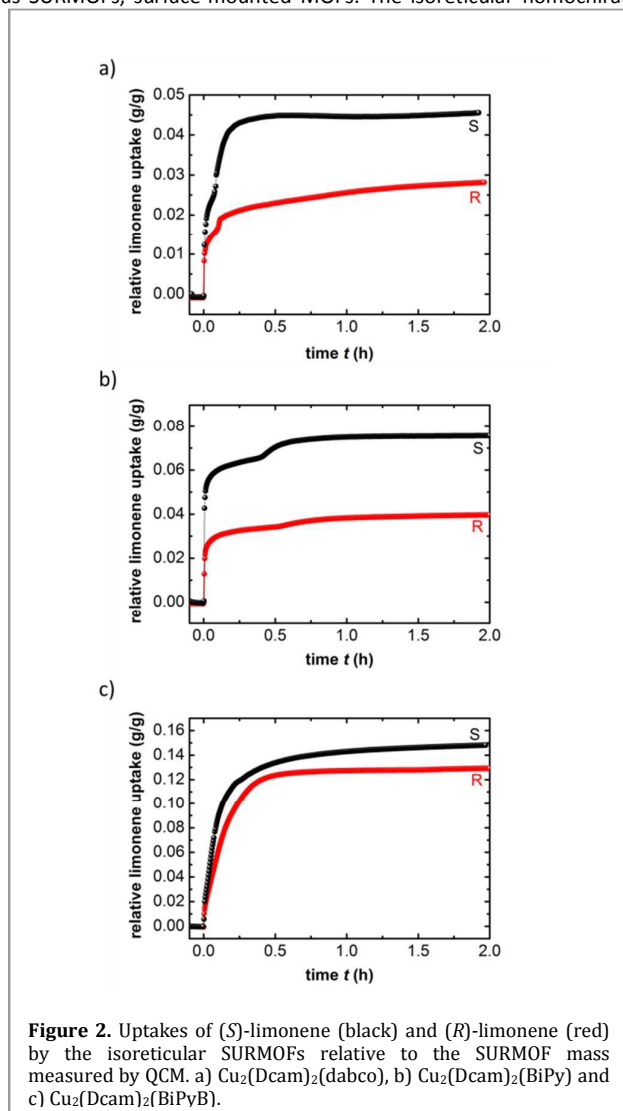
<sup>c</sup> Prof. Dr. S. Bräse, Institute of Organic Chemistry (IOC), Karlsruhe Institute of Technology (KIT), Fritz-Haber-Weg 6, 76131 Karlsruhe, Germany.

Electronic Supplementary Information (ESI) available: [details of any supplementary information available should be included here]. See DOI: 10.1039/x0xx00000x

For this purpose, the enantioselectivity during the adsorption of chiral probe molecules, (*R*)- or (*S*)-limonene, in an isorecticular series of homochiral pillared-layer MOFs of type  $\text{Cu}_2(\text{Dcam})_2(\text{L})^{28}$  with identical chiral (1*R*,3*S*)-(+)-camphoric acid (Dcam) layer linker and different pillar linkers L is studied, see figure 1. The pillar linkers L are N-donor ligands of type diazabicyclo[2.2.2]octane (dabco), 4,4'-bipyridyl (BiPy) and 1,4-bis(4-pyridyl)benzene (BiPyB) (see SI1), respectively. They are coordinated to the axial positions of the copper complexes, forming pillars of different length, perpendicular to the chiral  $\text{Cu}_2(\text{Dcam})_2$  layers. The lattice distances are 0.95 nm in [100] and [010] direction as well as 0.95 nm, 1.4 nm and 1.8 nm in [001] direction for the  $\text{Cu}_2(\text{Dcam})_2(\text{dabco})$ ,  $\text{Cu}_2(\text{Dcam})_2(\text{BiPy})$  and  $\text{Cu}_2(\text{Dcam})_2(\text{BiPyB})$  MOFs, respectively (Figure 1). This corresponds to pore sizes of roughly 0.7 nm in [100] and [010] directions and roughly 0.4 nm, 0.8 nm and 1.2 nm, respectively, in [001] direction. For a better quantification and the option to perform the adsorption experiments in a fast and straightforward fashion, we used thin films of MOFs prepared by liquid-phase epitaxy in a well-defined layer-by-layer fashion.<sup>29, 30</sup> These thin films are referred to as SURMOFs, surface-mounted MOFs. The isorecticular homochiral

SURMOFs were grown on gold-coated quartz crystal microbalance (QCM) sensors functionalized with 11-mercapto-1-undecanol (MUD) self-assembled monolayers (SAMs), resulting in a [001] crystal orientation of the SURMOF perpendicular to the substrate surface. The SURMOF samples were synthesized in QCM flow cells by pumping subsequently the ethanolic solution of 1 mM copper(II)acetate ( $\text{Cu}(\text{OAc})_2$ ) and 0.2 mM equimolar  $\text{H}_2\text{Dcam}$  and L (L = dabco, BiPy or BiPyB) through the cells. In between, the samples were purged with ethanol to remove unreacted, weakly absorbed reactants. The SURMOF masses (per area) were determined by QCM to  $10.8 \mu\text{g cm}^{-2}$ ,  $13.0 \mu\text{g cm}^{-2}$  and  $11.0 \mu\text{g cm}^{-2}$  (see SI2), respectively (which correspond to thicknesses of roughly 80 nm). The [001] growth orientation and the high crystallinity of the isorecticular chiral SURMOFs are shown by X-ray diffraction (SI3). All samples were additionally characterized by infrared spectroscopy (SI4).

A pair of chiral probe molecules, (*S*)- and (*R*)-limonene, was chosen to systematically investigate the relationship between enantioselectivities and pore sizes of the isorecticular homochiral SURMOFs. For this purpose, the uptake of the probe molecules by



the different SURMOF samples was studied employing a QCM.<sup>31, 32</sup> After activating the samples at 338 K in a flow of argon (99.9999% purity, 100 ml min<sup>-1</sup>) over night, the uptakes of the enantiopure guest molecules were studied from the gas phase at a temperature of 303 K. The initially pure argon was switched to an argon flow passing over (*R*)- or (*S*)-limonene at room temperature (298 K), resulting in an argon flow enriched with the vapor of the chiral guest molecule. The uptakes by the three different SURMOFs are studied in parallel at the same time to ensure identical conditions during the experiments. The uptakes of (*R*)- and (*S*)-limonene were investigated alternatively five times to guarantee reproducible results. Typical curves of the uptake of (*S*)- or (*R*)-limonene by the isorecticular homochiral SURMOFs are shown in Figure 2.

These QCM uptake curves enable the determination of the adsorption concentrations, Figure 3a. It is clearly visible that the adsorption capacity does not only change with the probe molecules but also with the MOF structure. The smallest adsorption capacity was determined for the SURMOF with the smallest pores (Cu<sub>2</sub>(Dcam)<sub>2</sub>(dabco)). For (*S*)-limonene, the loading is twice as much in Cu<sub>2</sub>(Dcam)<sub>2</sub>(BiPy) and three-times as much in the Cu<sub>2</sub>(Dcam)<sub>2</sub>(BiPyB) than in Cu<sub>2</sub>(Dcam)<sub>2</sub>(dabco). The loadings of (*R*)-limonene are smaller than that of (*S*)-limonene, in particular in Cu<sub>2</sub>(Dcam)<sub>2</sub>(BiPy). An increasing loading with increasing pore size can also be observed for (*R*)-limonene, verifying the fact that the SURMOFs are not interpenetrated.<sup>33</sup> From the uptake curve, kinetic parameters like the diffusion coefficient can also be determined.<sup>34, 35</sup> Since there are no significant differences between the different enantiomers, we did not focus on the kinetics. (Due to the small size of the pore windows in (001) direction,<sup>28</sup> it may be assumed that the uptake occurs along (100) and (010) directions, where the molecules enter from the side at defects like domain boundaries.)

The determined loadings of the molecules allow the calculation of the theoretically-possible enantiomeric excess, that would be obtained for a mixture of (*R*)- and (*S*)-limonene if there is no interaction between the different enantiomers, Fig. 3b. This means it corresponds to the enantiomeric excess at very low concentrations. It was found that the (theoretical) enantiomeric excess of (*S*)-limonene versus (*R*)-limonene changes significantly for the different MOF structures; namely approximately 8% for Cu<sub>2</sub>(Dcam)<sub>2</sub>(BiPyB), 17% for Cu<sub>2</sub>(Dcam)<sub>2</sub>(dabco) and 35% for Cu<sub>2</sub>(Dcam)<sub>2</sub>(BiPy).

The reliability of the data is checked by carrying out the experiments with SURMOFs of type Cu<sub>2</sub>(Lcam)<sub>2</sub>(BiPy), the enantiomeric mirror image of Cu<sub>2</sub>(Dcam)<sub>2</sub>(BiPy). The QCM data (SI5) show that the (theoretical) enantiomeric excess of (*R*)-limonene versus (*S*)-limonene is 34%, which is in perfect agreement with the data determined for Cu<sub>2</sub>(Dcam)<sub>2</sub>(BiPy).

The data show clearly that the pore size has a significant impact on the enantioselectivity. The enantioselectivity does not follow such a simple trend as the adsorption capacity, which increases with increasing pore size. The highest enantiomeric excess was found for a pore size of 0.8 nm, which was found to be the medium case. It can be assumed that the differences of the loadings are caused by the different alignments of the chiral guest molecules adsorbed in the pores, where the stereogenic centers have a different impact on the enantiomer selectivity. As visualization, Figure 4 shows a sketch of (*S*)-limonene in the isorecticular homochiral MOFs. This can be

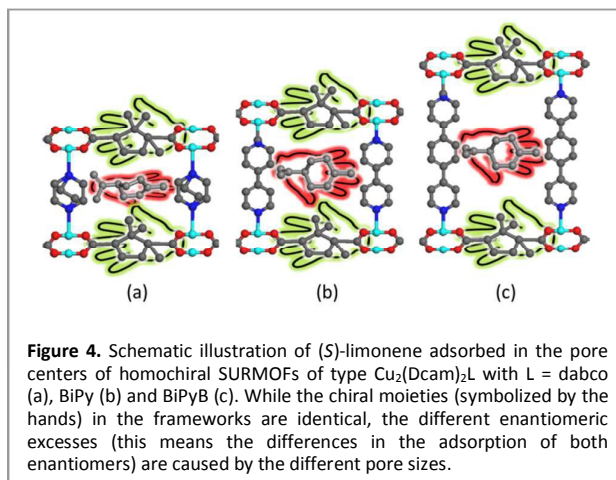


**Figure 4.** Schematic illustration of (*S*)-limonene adsorbed in the pore centers of homochiral SURMOFs of type Cu<sub>2</sub>(Dcam)<sub>2</sub>L with L = dabco (a), BiPy (b) and BiPyB (c). While the chiral moieties (symbolized by the hands) in the frameworks are identical, the different enantiomeric excesses (this means the differences in the adsorption of both enantiomers) are caused by the different pore sizes.

interpreted in the following way: If the pore size is “too” small (a), the guest molecules are “forced” to adsorb in the pores in such a position, where the impact of the stereogenic center in the framework is small. If the pore size is “too” large (c), the molecules can adsorb all over the large pore and the impact of the stereogenic center is small, too. If the pore size is well adjusted, roughly as large as the guest molecule (b), the stereogenic center has the highest impact on the guest molecule, resulting in the highest enantiomer separation.

In conclusion, the enantioselectivity of isorecticular chiral MOFs with identical stereogenic centers and different pore sizes was investigated. The enantioselective uptake of the chiral probe molecules, (*R*)- and (*S*)-limonene, by thin MOF films of type Cu<sub>2</sub>(Dcam)<sub>2</sub>(dabco), Cu<sub>2</sub>(Dcam)<sub>2</sub>(BiPy) and Cu<sub>2</sub>(Dcam)<sub>2</sub>(BiPyB) was measured by using a QCM. It was found that the adsorption capacity increases with increasing pore size. A more complex situation was found for the enantiomer selectivity, where the highest enantiomeric excess is in SURMOFs with medium pore size, while the enantiomeric excess for very small and large pores is significantly smaller. This study demonstrates that not only the stereogenic center, but also the pore size have to be adjusted for gaining highest enantioselectivities in chiral nanoporous materials and thereupon enabling a significantly more efficient enantiomer separation.

## References

1. A. M. Stalcup, in *Annual Review of Analytical Chemistry*, Vol 3, eds. E. S. Yeung and R. N. Zare, Annual Reviews, Palo Alto, 2010, vol. 3, pp. 341-363.
2. Y. Liu, W. Xuan and Y. Cui, *Adv. Mater.*, 2010, **22**, 4112-4135.
3. M. Padmanaban, P. Muller, C. Lieder, K. Gedrich, R. Grunke, V. Bon, I. Senkowska, S. Baumgartner, S. Opelt, S. Paasch, E. Brunner, F. Glorius, E. Klemm and S. Kaskel, *Chemical Communications*, 2011, **47**, 12089-12091.
4. X. J. Li, C. L. Chang, X. Wang, Y. Bai and H. W. Liu, *Electrophoresis*, 2014, **35**, 2733-2743.
5. H. C. Zhou, J. R. Long and O. M. Yaghi, *Chemical Reviews*, 2012, **112**, 673-674.

6. P. Horcajada, R. Gref, T. Baati, P. K. Allan, G. Maurin, P. Couvreur, G. Ferey, R. E. Morris and C. Serre, *Chemical Reviews*, 2012, **112**, 1232-1268.
7. S. Bureekaew, S. Shimomura and S. Kitagawa, *Science and Technology of Advanced Materials*, 2008, **9**.
8. T. Ezuhara, K. Endo and Y. Aoyama, *J. Am. Chem. Soc.*, 1999, **121**, 3279-3283.
9. G. Nickerl, A. Henschel, R. Gruncker, K. Gedrich and S. Kaskel, *Chem. Ing. Tech.*, 2011, **83**, 90-103.
10. K. Mo, Y. H. Yang and Y. Cui, *J. Am. Chem. Soc.*, 2014, **136**, 1746-1749.
11. M. M. Wanderley, C. Wang, C. D. Wu and W. B. Lin, *J. Am. Chem. Soc.*, 2012, **134**, 9050-9053.
12. M. Hatano and K. Ishihara, *Chemical Communications*, 2012, **48**, 4273-4283.
13. Z.-G. Gu, J. Bürck, A. Bihlmeier, J. Liu, O. Shekhah, P. G. Weidler, C. Azucena, Z. Wang, S. Heissler, H. Gliemann, W. Kloppner, A. S. Ulrich and C. Wöll, *Chemistry – A European Journal*, 2014, **20**, 9879-9882.
14. N. Marets, V. Bulach and M. W. Hosseini, *New J. Chem.*, 2013, **37**, 3549-3558.
15. R. E. Morris and X. Bu, *Nature Chemistry*, 2010, **2**, 353-361.
16. K. K. Bisht and E. Suresh, *J. Am. Chem. Soc.*, 2013, **135**, 15690-15693.
17. M. Cakici, Z.-G. Gu, M. Nieger, J. Burck, L. Heinke and S. Bräse, *Chemical Communications*, 2015, **51**, 4796-4798.
18. Y. Peng, T. Gong, K. Zhang, X. Lin, Y. Liu, J. Jiang and Y. Cui, *Nature Communications*, 2014, **5**.
19. L. Ma, C. Abney and W. Lin, *Chemical Society Reviews*, 2009, **38**, 1248-1256.
20. Q. Wei, H. W. Xu, X. H. Yu, T. Shimada, M. S. Rearick, D. D. Hickmott, Y. S. Zhao and S. N. Luo, *Journal of Applied Physics*, 2011, **110**.
21. D. Britt, D. Tranchemontagne and O. M. Yaghi, *Proc. Natl. Acad. Sci. U. S. A.*, 2008, **105**, 11623-11627.
22. S. Jeong, D. Kim, S. Shin, D. Moon, S. J. Cho and M. S. Lah, *Chem. Mat.*, 2014, **26**, 1711-1719.
23. D. N. Dybtsev, M. P. Yutkin and V. P. Fedin, *Russian Chemical Bulletin*, 2009, **58**, 2246-2249.
24. L. Ma, J. M. Falkowski, C. Abney and W. Lin, *Nature Chemistry*, 2010, **2**, 838-846.
25. D. N. Dybtsev, M. P. Yutkin, D. G. Samsonenko, V. P. Fedin, A. L. Nuzhdin, A. A. Bezrukov, K. P. Bryliakov, E. P. Talsi, R. V. Belosludov, H. Mizuseki, Y. Kawazoe, O. S. Subbotin and V. R. Belosludov, *Chemistry-a European Journal*, 2010, **16**, 10348-10356.
26. M. C. Das, Q. Guo, Y. He, J. Kim, C.-G. Zhao, K. Hong, S. Xiang, Z. Zhang, K. M. Thomas, R. Krishna and B. Chen, *J. Am. Chem. Soc.*, 2012, **134**, 8703-8710.
27. S.-C. Xiang, Z. Zhang, C.-G. Zhao, K. Hong, X. Zhao, D.-R. Ding, M.-H. Xie, C.-D. Wu, M. C. Das, R. Gill, K. M. Thomas and B. Chen, *Nature Communications*, 2011, **2**.
28. D. N. Dybtsev, M. P. Yutkin, E. V. Peresypkina, A. V. Virovets, C. Serre, G. Ferey and V. P. Fedin, *Inorganic Chemistry*, 2007, **46**, 6843-6845.
29. O. Shekhah, H. Wang, S. Kowarik, F. Schreiber, M. Paulus, M. Tolan, C. Sternemann, F. Evers, D. Zacher, R. A. Fischer and C. Wöll, *J. Am. Chem. Soc.*, 2007, **129**, 15118-15119.
30. L. Heinke, M. Tu, S. Wannapaiboon, R. A. Fischer and C. Wöll, *Microporous and Mesoporous Materials*, in press.
31. L. Heinke and C. Wöll, *Physical Chemistry Chemical Physics*, 2013, **15**, 9295-9299.
32. B. Liu, O. Shekhah, H. K. Arslan, J. X. Liu, C. Wöll and R. A. Fischer, *Angewandte Chemie-International Edition*, 2012, **51**, 807-810.
33. O. Shekhah, H. Wang, M. Paradinas, C. Ocal, B. Schupbach, A. Terfort, D. Zacher, R. A. Fischer and C. Wöll, *Nat Mater*, 2009, **8**, 481-484.
34. L. Heinke, Z. Gu and C. Wöll, *Nat Commun*, 2014, **5**.
35. L. Heinke and C. Wöll, *Physical Chemistry Chemical Physics*, 2013, **15**, 9295-9299.